Published in IEE Proceedings Vision, Image & Signal Processing, April, 2006, volume 153, issue 2, pag. 199-205, Digital Object Identifier 10.1049/ip-vis:20050213.

# Iris segmentation methodology for non-cooperative recognition

H. Proença and L.A. Alexandre

**Abstract:** An overview of the iris image segmentation methodologies for biometric purposes is presented. The main focus is on the analysis of the ability of segmentation algorithms to process images with heterogeneous characteristics, simulating the dynamics of a non-cooperative environment. The accuracy of the four selected methodologies on the UBIRIS database is tested and, having concluded about their weak robustness when dealing with non-optimal images regarding focus, reflections, brightness or eyelid obstruction, the authors introduce a new and more robust iris image segmentation methodology. This new methodology could contribute to the aim of non-cooperative biometric iris recognition, where the ability to process this type of image is required.

## 1 Introduction

The use of biometric systems has been increasingly encouraged by both government and private entities in order to replace or improve traditional security systems.

The iris is commonly recognised as one of the most reliable biometric measures: it has a random morphogenesis and no genetic penetrance. In 1987, Flom and Safir [1] studied the problem and concluded that iris morphology remains stable throughout human life and also estimated the probability of the existence of two similar irises on distinct persons at 1 in $10^{72}$.

The emerging needs for a safer and quicker access (buildings, weapons, restricted areas) requires non-cooperative techniques. In this paper, we consider a non-cooperative technique where the user has no active participation in the image-capture process and is not even aware of the recognition process.

As an example, we can think of a building access where users do not need to look through a small hole to have their irises recognised, but instead, an image-capture system captures the necessary information from their irises as they approach the door. This is much less invasive and will enable the dissemination of iris recognition systems to everyday applications.

Obviously, these image-capture conditions tend to acquire images with more heterogeneous characteristics with respect to reflection areas, brightness and contrast or focus conditions.

Having analysed the accuracy of some of the most cited iris image segmentation methodologies, we have concluded that they have small tolerance to image noise and thus are inappropriate for the application on non-cooperative recognition systems.



*IEE Proceedings* online no. 20050213

doi:10.1049/ip-vis:20050213

Paper first received 22nd July and in revised form 14th September 2005

The authors are with the Department of Informatics, IT – Networks and Multimedia Group, Universidade da Beira Interior, Covilhã, R. Marquês D'Avila e Bolama, 6200-001 Covilhã, Portugal

E-mail: hugomcp@di.ubi.pt

Our aim is to develop a new iris image segmentation methodology with a more robust behaviour. In order to do this, we use the UBIRIS [2] database, which contains very heterogeneous images and images with several types of noise, simulating the image capture without user cooperation.

### 1.1 Non-cooperative recognition

Despite the fact that many of the iris recognition approaches obtain minimal error rates, they do so under particularly favourable conditions, having as a prerequisite the existence of good quality images. These conditions are not easy to obtain and usually require the active cooperation of subjects, subjecting them to a slow and uncomfortable image-capture process.

We can easily anticipate some of the advantages of a non-cooperative iris recognition system.

- *Security:* As no cooperation is needed, the users do not have to know the location of the image-capture framework. Obviously, it is much more difficult to deceive a system when the subject does not know when and where the system is doing the recognition task.
- *User commodity:* The users' cooperation on the image-capture process lasts several seconds and it is often necessary to repeat the process. The fact that the users will not have to do this task will increase their commodity.
- *Total recognised persons:* Non-cooperative recognition systems will have a higher functioning radius than that of cooperative systems (usually less than 1 m). More time for the recognition task will increase the number of recognised persons.

It is obvious that this kind of system will require a complementary image-capture framework and computer vision techniques that can identify the person's silhouette, localise face and eye regions of the subject and provide the images from each of the subject's eyes. These systems are presently functioning for several other purposes and should not constitute an obstacle for non-cooperative iris recognition.

The dynamic conditions of such a non-cooperative environment induces the captured images to have more

heterogeneous characteristics regarding focus, contrast, brightness, reflections and eyelid or eyelashes obstruction parameters. It is important that the segmentation algorithms can adapt to such conditions and do not decrease their accuracy significantly.

## 2 Iris image segmentation methodologies

Since 1987, when the first relevant methodology was presented by Flom and Safir [1], many distinct approaches have been proposed. In 1993, Daugman [3] presented one of the most relevant methodologies, constituting the basis for many functioning systems. In the segmentation stage, this author introduced an integrodifferential operator to find both the iris inner and outer borders. This operator remains actual and was proposed with some minor differences in 2004 by Nishino and Nayar [4].

In a similar form, Camus and Wildes [5] and Martin-Roche *et al.* [6] propose integrodifferential operators that search over an $N^3$ space having as a objective the maximisation of equations that identify the iris borders. Wildes [7] proposed iris segmentation through a gradient-based binary edge-map construction followed by circular Hough transform. This is the most common methodology, being proposed with several minor variants in [8–13].

Liam *et al.* [14] have proposed a simple method on the basis of threshold and function maximisation in order to obtain two ring parameters corresponding to the iris inner and outer borders.

Du *et al.* [15] have proposed an iris detection method on the basis of prior pupil identification. The image is then transformed into polar coordinates and the iris outer border is identified as the largest horizontal edge resultant from Sobel filtering. This approach may fail in the case of non-concentric iris and pupil, as well as in very dark iris textures.

Morphologic operators were applied by Mira and Mayer [16] to obtain iris borders. They detect the inner border by applying threshold and image opening and closing and the outer border by applying image threshold, closing and opening sequences. On the basis of the assumption that the image-captured intensity values can be well represented by a mixture of three Gaussian distribution components, Kim *et al.* [17] have proposed the use of the expectation–maximisation algorithm [18] to estimate the respective distribution parameters. They expect that 'dark', 'intermediate' and 'bright' distributions contain the pixels corresponding to the pupil, iris and reflection areas.

The analysis of the iris recognition literature allowed us to identify two major strategies for iris segmentation: using a rigid or deformable template of the iris or its boundary. In most cases, the boundary approach is very similar to that of Wildes: it begins by the construction of an edge map followed by the application of some geometric form fitting algorithm. The template-based strategy usually involves the maximisation of some equations and is in general more specific.

Based on these facts, we selected four from these methodologies: the classical boundary-based Wildes' approach and three of the template approaches (Daugman's, Camus and Wildes' and Martin-Roche *et al.*'s). These were chosen because of their relevance in the literature, the results presented by the authors and by our belief that they are representative of the majority of the earlier-described methodologies.

The next sections detail the four selected methodologies, which were implemented and tested on the UBIRIS database.

### 2.1 Daugman's method

This methodology [3] is clearly the most cited in iris recognition literature. It is licensed to Iridian Technologies who turned it into the basis for 99.5% of the present-day commercial iris recognition systems. Proposed in 1992, it was the first methodology effectively implemented in a working biometric system.

Daugman [3] assumed both pupil and iris with a circular form and applied an integrodifferential operator

$$\max_{r,x_0,y_0} \left| \boldsymbol{G}_\sigma(r) * \frac{\partial}{\partial r} \oint_{r,x_0,y_0} \frac{I(x,y)}{2\pi r} \mathrm{d}s \right| \qquad (1)$$

This operator searches over the image domain $(x, y)$ for the maximum in the blurred (by a Gaussian kernel $G_\sigma(r)$) partial derivative with respect to increasing radius $r$, of the normalised contour integral of $I(x, y)$ along a circular arc d$s$ of radius $r$ and centre coordinates $(x_0, y_0)$. In practical terms, this method searches in an $N^3$ space for the circumference centre and radius that have the highest derivative value when compared with that of neighbour radius. This process, as shown in Section 5.2, proved to be very effective on images with clear intensity separability between iris, pupil and sclera regions.

However, we observed that it frequently fails when images do not have sufficient intensity separability between iris and sclera regions. As possible optimisations, we implemented two pre-process operations that enhanced image contrast and contributed to the improvement of the results (Section 5.2).

- *Histogram equalisation:* This operation improves the contrast between each eye's region, thus contributing to the correct algorithm segmentation.
- *Binarisation:* Applying a threshold on an image before the operator's execution enables the maximisation of the contrast between the regions belonging to the iris and the remaining ones. This process has, however, one major disadvantage: it is highly dependent on the threshold chosen and as image characteristics may change, the results may seriously deteriorate. Apart from this fact, the binarisation compromises one of this methodology's biggest advantages: the inexistence of user-defined parameters for the segmentation task.

### 2.2 Wildes' method

This methodology, proposed in 1997 by Wildes [7], performs its contour fitting in two steps. First, the image intensity information is converted into a binary edge map. Second, the edge points vote to instantiate particular contour parameter values.

The construction of the edge map is accomplished through the gradient-based Canny edge detector. In order to incorporate directional tuning, the image intensity derivatives are weighted to favour ranges of orientation. For example, on the iris/sclera border, the derivatives are weighted to be selective for vertical edges.

The second step is made through the well-known circular Hough transform where each edge point votes for particular contour parameter values.

This methodology is clearly the most common in iris segmentation approaches, having as a principal disadvantage the dependence of threshold values on the edge-map construction. This fact can obviously constitute one weak point as far as the robustness is concerned and includes the ability to deal with heterogeneous image characteristics.

Regarding this methodology, we observed that the edge-detector algorithm and the necessary tuned parameters are critical factors for its accuracy. We tested this methodology with three distinct and well-known edge-detector algorithms: Canny, Shen and Castan and zero-crossing.

### 2.3 Camus and Wildes' method

Camus and Wildes [5] described an algorithm for finding a subject's iris in a close-up image. In a way similar to Daugman's methodology [3], their algorithm searches in an $N^3$ space for the three circumference parameters (centre $(x, y)$ and radius $z$) by maximising the following function

$$C = \sum_{\theta=1}^{n}\left((n-1)\|g_{\theta,r}\| - \sum_{\phi=\theta+1}^{n}\|g_{\theta,r} - g_{\phi,r}\| - \frac{I_{\theta,r}}{n}\right) \quad (2)$$

where $n$ is the total number of directions and $I_{\theta,r}$ and $g_{\theta,r}$ are, respectively, the image intensity and derivatives with respect to the radius in the polar coordinate system.

This methodology (see Section 5.2) is very accurate on images where the pupil and iris regions' intensities are clearly separated from the sclera ones and on images that contain no reflections or other noise factors. When dealing with noisy data, the algorithm's accuracy deteriorates significantly.

### 2.4 Martin-Roche et al.'s method

This methodology, proposed in [6], operates in a way similar to Daugman's. It receives a grey-scale image, applies the histogram stretch and tries to maximise the average intensity differences of the five consecutive circumferences, defined as

$$D = \sum_{m}\left(\sum_{K=1}^{5}(I_{n,m} - I_{n-k,m})\right) \quad (3)$$

where $I_{i,j} = I(x_0 + i\Delta_r \cos(j\Delta_\Theta), y_0 + I\Delta_r \sin(j\Delta_\Theta))$. $\Delta_r$ and $\Delta_\Theta$ are the increments of radius and angle, respectively, and $I(x, y)$ is the image intensity.

In practical terms, this method finds three $N^3$ circumference parameters (centre $(x, y)$ and radius $r$), where the intensity difference between five successive circumferences is maximal.

## 3 Proposed methodology

As described in Section 2, common iris segmentation methodologies either apply an edge-detector operator for the edge-map construction or analyse the intensity derivatives with respect to the radius of consecutive circumferences. Both situations are dependent on the specific image characteristics, its brightness and contrast, as well as the existence of noise factors (reflections, eyelids or eyelashes, iris obstruction, and so on).

The development of a new iris segmentation methodology with robust behaviour in the presence of heterogeneous and noisy images begins with the identification of a feature set less dependent on particular image characteristics and noise factors. This feature set should contain enough information to separate the pixels belonging to the iris from the remaining ones.

Moment functions are widely used in various realms of computer vision and image processing. Numerous algorithms and techniques have been developed using image moments in the area of pattern recognition. Tuceryan [19] found that the computed image moments could capture important textural properties of images and some of the tested images were very similar in terms of the texture to those contained in UBIRIS.

For these reasons, we have evaluated the accuracy of the segmentation process proposed by Tuceryan [19] on the UBIRIS database and used this process as the basis for the development of a more accurate and robust iris image segmentation methodology.

### 3.1 Tuceryan's methodology

Tuceryan [19], proposed a moment-based texture segmentation algorithm, using the moments in small windows of the image as texture features and then applying a clustering algorithm to segment the image. The second-order regular geometric moments for each pixel in the image are computed using

$$M_{pq} = \sum_{-W/2}^{W/2}\left(\sum_{-W/2}^{W/2}(I(m, n)x_m^p y_n^q)\right) \quad (4)$$

where $M_{pq}$ is the regular geometric moment of order $pq$, $I(m, n)$ the pixel image intensity, $x$, $y$ the neighbourhood window coordinates and $W$ the width.

Tuceryan [19] concluded that these regular moments did not have sufficient discriminant capacity and proposed the application of the hyperbolic tangent as a non-linear transducer followed by an averaging step

$$F_{pq}(i, j) = \frac{1}{L^2}\sum_{(a,b)\in W_{ij}}\left(\tanh(\sigma(M_{pq}(a, b) - \bar{M}))\right) \quad (5)$$

where $F_{pq}$ is the feature image of the $M_{pq}$ moments with mean $\bar{M}$ and $W_{ij}$ is an $L \times L$ average window centred at location $(i, j)$. $\sigma$ is a parameter that controls the shape of the logistic function and was determined, by trial and error, as 0.01 for most cases.

At the classification stage, the well-known clustering $K$-means algorithm is applied producing as output the $n$ clusters-labelled image.

### 3.2 Our methodology

Our segmentation algorithm is given in the block diagram of Fig. 1. The essential point consists in making the edge-map construction less dependent on the specific image characteristics. A normalised (clustered) intermediate image is produced that will be used for the edge-map construction.

The process begins with the image-feature extraction where three discrete values are extracted for each image pixel, followed by the application of a clustering algorithm that will label (classify) each pixel and produce the intermediate image.

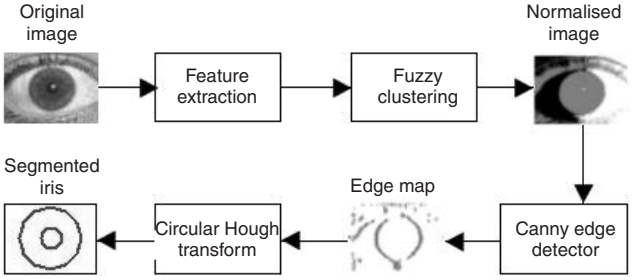


**Fig. 1** *Proposed methodology block diagram*

This image is then used by the edge-detector algorithm and, as it has more homogeneous characteristics, facilitates the tuning of the parameters required by the edge-detector algorithm. A more accurate edge map enables a higher accuracy of the circular Hough transform in its circumference detection task.

*3.2.1 Feature extraction:* We did several tests to select the best feature set and evaluate which set could simultaneously and clearly identify the iris regions and minimise the noisy information related to eyelashes and eyelids (Fig. 2).

We concluded that three discrete components $\{x, y, z\}$, being $(x, y)$ the coordinates of the pixel position on the image and $z$ the correspondent pixel image intensity, can characterise each pixel and enable a correct segmentation. This feature set, hereinafter named 'Pixel position + intensity', preserves information about the spatial relations in the image as well as about the individual properties of each pixel.

The moments $F_{20}$ and $F_{02}$ proved to correctly identify the iris border but also produced considerable noise regarding the eyelid regions. This noise is an important obstacle to the posterior circumference detection stage.

*3.2.2 Clustering algorithm:* For the clustering (classification) algorithm, the most important feature is its capacity to classify, in the same class, all the pixels belonging to the iris and all the remaining ones in a distinct one. For this purpose, we evaluated four unsupervised clustering and classification algorithms:

*Kohonen's self-organising maps:* Also called topological ordered maps, the goal of this algorithm is to represent all points in the source space by points in the target space, such that distance and proximity relationships are preserved as much as possible. The task is this: having an input space $\phi$ and a sequence of input points, to create a mapping from $\phi$ to the target space $y$ such that points neighbouring in the source space are mapped to points that are neighbouring in $y$. The map is usually learned by a fully connected neural network where each cell represents a point in the target space. When a pattern from $\phi$ is presented, each cell in the target space computes its net activation and one of the cells is activated. All weights from this cell and its neighbours are then adjusted in relation to the input pattern.

*K-means:* Having a predefined number of $k$ clusters and $n$ data points, each one with dimension $d$, the algorithm begins by randomly initialising each coordinate of the $k$ clusters. The distance between data points and clusters is computed and each input corresponds to one activated cluster. The weights of this cluster are adjusted in relation to the input so that at the end of each iteration, the distance between data points and clusters is minimal. This process is repeated iteratively until the cluster weights are not adjusted. At this point, the $k$ clusters are returned as the algorithm output.

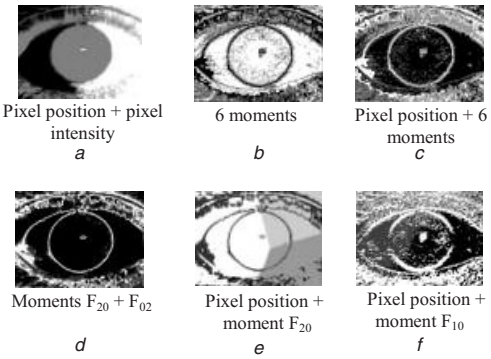


**Fig. 2** *Tested feature sets*

*Fuzzy K-means:* In every iteration of the classical $k$-means procedure, each data point is assumed to belong exactly and completely to one cluster. Relaxing this condition, we can think that each sample has a fuzzy membership to each of the $k$ clusters. These memberships are equivalent to the probabilities $\hat{P}(w_i|x_j, \hat{\boldsymbol{\theta}})$, where $\hat{\boldsymbol{\theta}}$ is the parameter vector for the membership functions. The fuzzy $k$-means clustering algorithm seeks a minimum of a heuristic global cost function $J_{\text{fuz}}$ [20]

$$J_{\text{fuz}} = \sum_{i=1}^{c}\left(\sum_{j=1}^{n}(\hat{P}(w_i|x_j,\hat{\boldsymbol{\theta}})^b \|x_j - \mu_i\|^2)\right) \tag{6}$$

where $b$ is a free parameter chosen to adjust the blending of different clusters. In practical terms, for each input presented, all the clusters will have to adjust their weights, regarding the distance between the input and the cluster weights, which are the probabilities that the input belongs to each cluster.

*Expectation–maximisation:* The basic idea of this algorithm is to iteratively estimate the likelihood, given the data that are present. Suppose $x_i$ is the $i$th observation of the random variable $X$. Let $f_j(x|\theta_j)$, $1 \le j \le L$, be a set of $L$ density functions, each having its parameter set $\theta_j$. The density function of the random variable $X$ can be modelled as a weighted sum of the $L$ density functions as

$$f(x|\theta) = \sum_{j=1}^{L}(\pi_j f_j(x|\theta_j)) \tag{7}$$

where $\pi_j$, $1 \le j \le L$, are the weights. The aim of the maximum-likelihood (ML) estimation is to find the set of $\theta$ and $\pi$ that maximises the likelihood function $P(x)$ with respect to the given data $x_i$

$$P(x) = \prod_{i=1}^{N}\left(\sum_{j=1}^{L}(\pi_j f_j(x|\theta_j))\right) \tag{8}$$

The observed data are supposed to be a subset of the complete data $y$. The expectation–maximisation algorithm starts by using an initial estimate $\hat{\boldsymbol{\theta}}^0$ before performing the following two steps at each iteration:

*expectation step:*

$$Q(\theta, \hat{\boldsymbol{\theta}}|\theta^p) = E(\log f(y|\theta)|x, \hat{\boldsymbol{\theta}}^p); \quad \text{and}$$

*maximisation step:*

$$\hat{\boldsymbol{\theta}}^{p+1} = \arg\max_\theta Q(\theta|\hat{\boldsymbol{\theta}}^p)$$

Table 1 presents the results obtained for every feature set and the clustering (classification) algorithm tested. The information about the iris image data set and the way the results were obtained is detailed, respectively, in Sections 4.1 and 5.2.

These results led us to select the fuzzy $K$-means algorithm and the three discrete features: $(x, y)$ corresponding to the pixel position and $z$ to its intensity. As can be seen, considering all the evaluated algorithms, this configuration presents the smallest degradation between the first and second capture-session images, thus presenting a more tolerant behaviour and better capacity to deal with non-optimal data.

**Table 1: Variants of the proposed algorithm**

| Algorithm | Features | Session 1, % | Session 2, % |
|---|---|---|---|
| *K*-means | Pixels position + intensity | 97.69 | 96.83 |
| *K*-means | Moments $F_{20} + F_{02}$ | 92.33 | 89.14 |
| SOM | Pixels position + intensity | 97.69 | 96.68 |
| SOM | Moments $F_{20} + F_{02}$ | 95.14 | 90.95 |
| Fuzzy *K*-means | Pixels position + intensity | 98.02 | 97.88 |
| Fuzzy *K*-means | Moments $F_{20} + F_{02}$ | 93.90 | 90.04 |
| Expectation–maximisation | Pixels position + intensity | 96.86 | 95.17 |
| Expectation–maximisation | Moments $F_{20} + F_{02}$ | 92.17 | 89.14 |

## 4 Iris databases

Apart from UBIRIS, there are presently four public and freely available iris image databases:

*CASIA* [21]. This is the most widely used iris image database, having two distinct versions. The first version has one major disadvantage: the authors pre-processed the images such that the pupil region is identified and filled with black pixels. Some iris segmentation approaches profit from this pre-processing and improve their segmentation results. The second version does not have this disadvantage and introduces several noise factors, especially relative to eyelids and eyelashes obstruction and focus quality. However, we observed that almost all images appeared to be captured at similar lighting conditions, reducing its heterogeneity and the usefulness for the purpose of evaluating the robustness of segmentation algorithms.

*Multimedia University (MMU)* [22]. Images from this database present few noise factors and their characteristics are also very homogeneous. A fixed image-capture process must have been followed, clearly simulating a cooperative environment.

*University of Bath* [23]. Images from this database are quite similar to the ones contained in MMU. They have very similar characteristics and few noise factors, almost exclusively related with small eyelid or eyelashes obstructions.

*Lions Institute* [24]. These are by far the most homogeneous iris database images; thus it is less useful to our work purposes. All images were captured with an optometric framework resulting in optimal images with extremely similar characteristics.

### 4.1 UBIRIS database

The UBIRIS [2] database was built during September 2004. It comprised 1877 images captured from 241 persons in two distinct sessions: 1214 images in the first and 663 in the second.

For the first image-capture session (the enrolment), the noise factors were minimised, especially those relative to reflections, luminosity and contrast. In the second session, several noise factors were introduced, enabling the appearance of heterogeneous images regarding reflections, contrast, luminosity, eyelid and eyelash iris obstruction and focus characteristics.

All images from both sessions were manually classified with respect to three parameters ('focus', 'reflections' and 'visible iris') in a three values scale ('good', 'average' and 'bad').

Fig. 3 contains examples of UBIRIS images: (3*a*) and (3*b*) are good quality images, (3*c*), (3*d*), (3*e*) and (3*f*) are non-optimal images: poorly focused, with eyelid obstruction and with large reflection areas.

Table 2 contains the statistical information about the quality of the images from both sessions. Images from the first session typically have good quality, corresponding to images captured with the subject's cooperation. The second session contains a much higher number of non-optimal images, trying to simulate the non-cooperative capture, often obtaining images poorly focused, or with large reflection areas or with small visible iris areas due to eyelids or eyelashes obstruction.

## 5 Experiments

In this section, we justify the choice of the UBIRIS database and compare the results obtained between the methodologies described in Section 2 and our proposal.

### 5.1 Experiments' database

By examining the databases presented in Section 4 and their images, we concluded that they all simulate cooperative iris recognition processes, with fixed image-capture conditions and parameters. This fact explains why a large majority of their images present very homogeneous characteristics and few noise factors.

When compared with the other public iris image databases, the images from UBIRIS have much more heterogeneous characteristics. In addition, a significant part of the irises are obstructed by eyelids or eyelashes and some of the images have large reflection areas (Fig. 3*f*); thus introducing several parameters that can constitute obstacles to correct iris segmentation.

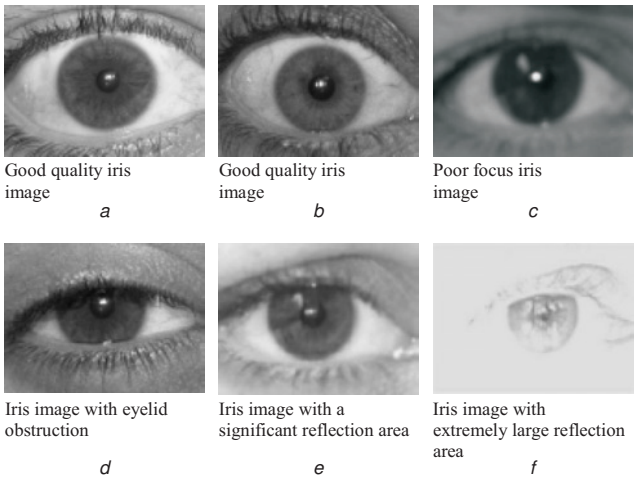


**Fig. 3** *Examples from UBIRIS images*

**Table 2: UBIRIS database statistics**

| Quality | Session 1 (%: good, average, bad) | Session 2 (%: good, average, bad) |
|---|---|---|
| Focus | (82.94, 13.67, 3.78) | (69.68, 19.45, 10.85) |
| Reflections area | (94.56, 2.80, 2.63) | (24.13, 38.61, 37.25) |
| Visible iris area | (89.29, 7.16, 3.45) | (22.32, 69.07, 8.59) |

Our work is focused on the analysis of the accuracy of the iris segmentation algorithms as image quality and characteristics change, simulating two distinct cooperative (enrolment stage) and non-cooperative (recognition stage) image-capture processes. The images' heterogeneity and the several noise factors were the main factors that led us to choose the UBIRIS database as the basis for our experiments.

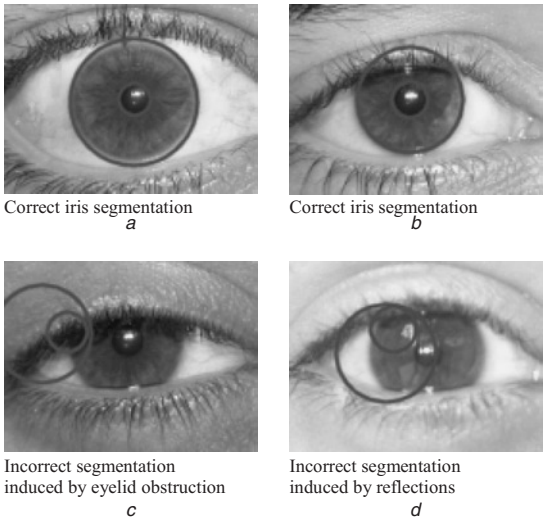


**Fig. 4** *Segmented images*

### 5.2 Results and discussion

Table 3 presents the results obtained by each described methodology. The first column identifies the method, the second specifies the eventual parameter modifications with respect to the original methodology, the third and fourth contain the accuracy results, respectively, on images from UBIRIS first and second sessions. These results correspond to 99% confidence interval and are in percentage. The fifth column shows accuracy deterioration from the first to second image-capture session and the last shows the averaged computation time for each methodology (Section 5.3).

These results were obtained by visual inspection of each segmented image. We consider a correct segmentation when the circumference parameters corresponding to the pupilar and scleric borders fall exactly into the respective borders as we can see on Figs. 4*a* and 4*b*. Figs. 4*c* and 4*d* exemplify incorrect segmentation processes because of eyelid obstruction or large reflection areas.

For our purposes, the most relevant result from Table 3 is the accuracy degradation as the image quality changes. We observed that the proposed methodology is clearly less dependent on image conditions, presenting the smallest accuracy degradation in the presence of noise factors. As can be seen, the observed accuracy degradation on the first and second session images was just about 0.14%, contrasting with all remaining methodologies, specially the methodologies proposed by Martin-Roche *et al.* [6], Daugman [3] and Camus and Wildes [5]. It should be noticed that our methodology is the one that presented the highest accuracy on images from session 2, indicating that it is well adapted to deal with noisy images.

Wildes' [7] methodology presented the best results in absolute terms, having 98.68% accuracy on the first session images. However, as the image quality decreases, its accuracy degraded more than 2%. This fact may indicate that, as we incorporate other noise factors, its accuracy will be affected, thus discouraging its use in a non-cooperative architecture framework. The two implemented variants of this method presented worst results than the original one.

Daugman's [3] methodology has one important advantage: it is not dependent on any parameter value. This fact may, in theory, potentiate its robustness, but the results showed that its accuracy is directly proportional to the image quality and the existence of sufficient intensity value separability between iris and sclera regions. Especially on irises with high-intensity values (blue or green eyes) where the intensity difference between the iris and sclera parts is not as large, the maximal difference between consecutive circumferences tends to identify regions tangent to the pupil region.

**Table 3: Iris segmentation results**

| Methodology | Parameters | Session 1, % | Session 2, % | Degradation, % | Time, s |
|---|---|---|---|---|---|
| Daugman | Original methodology | 95.22 $\pm$ 0.015 | 88.23 $\pm$ 0.032 | 6.99 | 2.73 |
| Daugman | Histogram equalisation pre-process | 95.79 $\pm$ 0.014 | 91.10 $\pm$ 0.028 | 4.69 | 3.01 |
| Daugman | Threshold pre-process (128) | 96.54 $\pm$ 0.013 | 95.32 $\pm$ 0.021 | 1.22 | 2.92 |
| Wildes | Original methodology | 98.68 $\pm$ 0.008 | 96.68 $\pm$ 0.017 | 2.00 | 1.95 |
| Wildes | Shen and Castan edge detector | 96.29 $\pm$ 0.013 | 95.47 $\pm$ 0.020 | 0.82 | 2.49 |
| Wildes | Zero-crossing edge detector | 94.64 $\pm$ 0.016 | 92.76 $\pm$ 0.025 | 1.88 | 2.51 |
| Camus and Wildes | Original methodology, number of directions = 8 | 96.78 $\pm$ 0.013 | 89.29 $\pm$ 0.030 | 7.49 | 3.12 |
| Martin-Roche *et al.* | Original methodology | 77.18 $\pm$ 0.030 | 71.19 $\pm$ 0.045 | 5.99 | 2.91 |
| Tuceryan | Total clusters = 5 | 90.28 $\pm$ 0.021 | 86.72 $\pm$ 0.033 | 3.56 | 4.81 |
| Proposed methodology | Fuzzy $K$-means + $(x, y)$ = position, $z$ = intensity | 98.02 $\pm$ 0.010 | 97.88 $\pm$ 0.015 | 0.14 | 2.30 |

Similar approaches to this methodology, such as the Camus and Wildes [5] and Martin-Roche *et al.* [6] ones, present similar error rates. These methodologies proved their effectiveness on good quality images but deteriorate significantly in their accuracy when images contain large reflection regions or eyelids obstruct a significant part of the iris.

Regarding the Tuceryan [19] methodology, the fact that it was not specifically proposed for iris recognition can probably explain why their average accuracy was about 7% worse than the specific iris segmentation methods. Apart from this fact, the accuracy degradation (around 4%) was in both cases more relevant when compared with that in other approaches. As Fig. 2 shows, we concluded that the geometric moments do not have sufficiently discriminant capacity to distinguish the iris regions; thus inducing, frequently, an incorrect segmentation.

### 5.3 Computation time

All the algorithms were implemented in C++, following an object-oriented paradigm and running in an image-processing framework developed by ourselves. This framework is clearly not optimised for execution speed as the algorithm's implementation was made without these concerns, but instead with a user-friendly objective.

The 'Time' column from Table 3 contains the average execution time from each of the segmentation processes tested. These time values were obtained by averaging 100 segmentation processes on 100 distinct UBIRIS images. Regarding these values, we observed that the classical edge detection followed by the circumference fitting (Wildes) algorithm is more efficient than all the remaining ones.

Our methodology computation time is about 17% superior to that of the Wildes' algorithm. This 17% is attributed to the feature extraction and clustering process. We think that with proper algorithm optimisation, this computation time gap (about 0.3 s) will become irrelevant.

## 6 Conclusions

We have described the problems associated with the segmentation of iris images with poor quality. We presented some of the most cited methodologies in the iris segmentation literature and used the UBIRIS [2] database to show that they are dependent on the specific image-capture conditions, yielding a low robustness level.

On the basis of this fact, we proposed a new iris segmentation methodology that consists of the selection of three discrete features followed by the application of the well-known fuzzy-clustering algorithm. This produces an intermediate image that tends to be more homogeneous even on images with very different focus, brightness or contrast characteristics. Results showed that for these non-optimal images, the creation of an intermediate labelled image improves the segmentation accuracy and is therefore adequate for the application on a non-cooperative iris recognition system.

## 7 References


1 Flom, L., and Safir, A.: 'Iris recognition system'. U.S. Patent 4641394, 1987

2 Proença, H., and Alexandre, L.A.: 'UBIRIS: a noisy iris image database'. ICIAP 2005, 13th Int. Conf. on Image Analysis and Processing, Cagliari, Italy, 6–8 September 2005, *Lect. Notes Comput. Sci.*, **3617**, pp. 970–977, ISBN 3-540-28869-4. http//iris.di.ubi.pt

3 Daugman, J.G.: 'High confidence visual recognition of persons by a test of statistical independence', *IEEE Trans. Pattern Anal. Mach. Intell.*, 1993, **15**, (11), pp. 1148–1161

4 Nishino, K., and Nayar, S.K.: 'Eyes for relighting', *ACM Trans. Graph*, 2004, **23**, (3), pp. 704–711, ISSN 0730-0301

5 Camus, T.A., and Wildes, R.: 'Reliable and fast eye finding in close-up images'. IEEE 16th Int. Conf. on Pattern Recognition, Quebec, Canada, 2004, pp. 389–394

6 Martin-Roche, D., Sanchez-Avila, C., and Sanchez-Reillo, R.: 'Iris recognition for biometric identification using dyadic wavelet transform zero-crossing', *IEEE Aerosp. Electron. Syst. Mag.*, 2002, **17**, (10), pp. 3–6

7 Wildes, R.P.: 'Iris recognition: an emerging biometric technology', *Proc. IEEE*, 1997, **85**, (9), pp. 1348–1363

8 Cui, J., Wang, Y., Tan, T., Ma, L., and Sun, Z.: 'A fast and robust iris localization method based on texture segmentation', 2004. http://nlpr-web.ia.ac.cn/english/irds/papers/cuijl/SPIE.pdf

9 Huang, J., Wang, Y., Tan, T., and Cui, J.: 'A new iris segmentation method for recognition'. Proc. 17th Int. Conf. on Pattern Recognition (ICPR04), Cambridge 2004, Vol. 3, pp. 554–557

10 Kong, W.K., and Zhang, D.: 'Accurate iris segmentation method based on novel reflection and eyelash detection model'. Proc. 2001 Int. Symp. on Intelligent Multimedia, Video and Speech Processing, Hong Kong, May 2001

11 Ma, L., Wang, Y., and Tan, T.: 'Iris recognition based on multichannel Gabor filtering'. ACCV2002: 5th Asian Conf. on Computer Vision, Melbourne, Australia, January 2002, Vol. 1, pp. 279–283

12 Ma, L., Tan, T., Wang, Y., and Zhang, D.: 'Personal identification based on iris texture analysis', *IEEE Trans. Pattern Anal. Mach. Intell.*, 2003, **25**, (12), pp. 1519–1533

13 Ma, L., Wang, Y., and Zhang, D.: 'Efficient iris recognition by characterizing key local variations', *IEEE Trans. Image Process.*, 2004, **13**, (6), pp. 739–750

14 Liam, L., Chekima, A., Fan, L., and Dargham, J.: 'Iris recognition using self-organizing neural network'. IEEE, 2002 Student Conf. on Research and Developing Systems, Malaysia, 2002, pp. 169–172

15 Du, Y., Ives, R., Etter, D., Welch, T., and Chang, C.: 'A new approach to iris pattern recognition'. SPIE European Symp. on Optics/Photonics in Defence and Security, London, UK, October 2004

16 Mira, J., and Mayer, J.: 'Image feature extraction for application of biometric identification of iris: a morphological approach'. IEEE Proc. XVI Brazilian Symp. on Computer Graphics and Image Processing (SIBGRAPI03), São Paulo, Brazil, 2003

17 Kim, J., Cho, S., and Choi, J.: 'Iris recognition using wavelet features', *J. VLSI Signal Process.*, 2004, **38**, (2), pp. 147–156

18 Dempster, A.P., Laird, N., and Rubin, D.: 'Maximum likelihood from incomplete data via the EM algorithm', *J. R. Stat. Soc.*, 1977, **39**, pp. 1–38

19 Tuceryan, M.: 'Moment based texture segmentation', *Pattern Recognit. Lett.*, 1994, **15**, pp. 659–668

20 Bezdek, R.C., Ehrlich, R., and Full, W.: 'FCM: the fuzzy *c*-means clustering algorithm', *Comput. Geosci.*, 1984, **10**, pp. 191–203

21 'CASIA iris image database', Chinese Academy of Sciences Institute of Automation, http://www.sinobiometrics.com

22 'MMU iris image database', Multimedia University, http://pesona.mmu.edu.my/~ccteo

23 'University of Bath iris image database', University of Bath, http://www.bath.ac.uk/elec-eng/pages/sipg/irisweb

24 Dobes, M., and Machala, L.: 'Iris database', Palacky University in Olomouc, Czech Republic, http://www.inf.upol.cz/iris/